JOURNAL OF MATERIALS SCIENCE 30 (1995) 4527–4534

Structural defects as a result of Zn diffusion into CdTe single crystals

M. AZOULAY, E. GROSSMAN, H. SCHACHAM, M. MIZRACHI, A. RAIZMAN
Solid State Physics Department, Soreq Nuclear Research Center, Yavne 81800, Israel

The presence of defects in CdZnTe crystals is detrimental for optoelectronic devices fabrication and therefore should be minimized. In this paper we present the characterization of structural defects on the surface and the cross-section of CdTe single crystals that were subjected to high temperature (up to 950 °C) diffusion of Zn. The defects were characterized by various X-ray techniques, optical microscopy, scanning electron microscopy (SEM) and atomic force microscopy (AFM). Quantitative data are obtained, a practical solution for reducing the defects is suggested and some implementations are discussed. Further effort is currently being made to investigate the lattice sites which are involved with the diffused Zn atoms near the surface and in the bulk.

1. Introduction

The study of the diffusion of Zn into CdTe crystals is of great interest for both fundamental and practical reasons. Such knowledge may contribute to a better understanding of the growth of CdZnTe crystals and to the development of CdZnTe components, such as the preparation of lattice matched CdZnTe substrates, from CdTe single crystals, for the growth of thin films. The diffusion process has been investigated and reported recently, the diffusion constants calculated [1, 2] and some thermomechanical effects observed, resulting in severe brittle fracture and ductile slip defects which were assessed by scanning electron microscopy. However, to the author's knowledge, no structural defects or morphological substructure formation as a result of the diffusion of Zn into CdTe crystals were reported up to date. The understanding of the defects associated with diffusion may lead to optimization of the process parameters, aimed at minimizing the dislocation density in the diffusion region, approaching crystalline perfection similar to the "mother phase" of the CdTe single crystal.

In the present work the published data [2] has been utilized to calculate predetermined diffusion curves that would provide the desired Zn content and crystalline perfection on the surface. In addition, structural defects on the diffused surface and cross-section have been studied by various X-ray techniques and different microscopy methods. These techniques were found to be complementary to each other by providing experimental data on both the morphological nature of the defects as well as giving a quantitative estimation on the density of dislocations and their distribution. For the first time, atomic force microscopy (AFM) was utilized with high resolution (nanoscale) to observe deformation patterns accompanying the Zn compositional distribution in the cross-sectional dimension of the diffusion on an "as-cleaved" (1 1 0) crystallographic plane, without any selective chemical surface treatment. A recent AFM study on as-cleaved surfaces of CdZnTe single crystals could only show cleavage steps and the deformation of the step structure as a result of annealing, but no substructure or structural defects [3]. Further study may be performed in order to distinguish between types of defects near the surface region and those in the bulk (remote from the surface).

2. Experimental procedure

CdTe single crystals were grown from the stoichiometric melt by the vertical gradient freeze (VGF) method. A detailed description of the growth process has been reported elsewhere [4]. Some of these crystals were utilized to prepare the samples for the diffusion experiments. CdTe (1 1 1) orientated slices, with an area of 10×10 mm and about 1.5 mm thick, were cut with a wire saw and then mechanochemically polished in a 5% bromine methanol solution.

A CdZn solution was selected as reservoir, providing the required Zn concentration and near equilibrium Cd vapour pressure. The CdZn reservoir and the CdTe sample were placed in two separate quartz containers that were loaded into a quartz ampoule, evacuated, sealed and then loaded to a horizontal furnace. The diffusion process was carried out in a three zone furnace, resistively heated, providing two different temperature regions, one for the sample and the other for the reservoir, respectively. After the diffusion process, the samples were cleaved on the $\{1\,1\,0\}$ crystallographic plane, parallel to the diffusion direction or alternatively were polished on the surface and then analysed.

The compositional analysis of Zn, Cd and Te was performed by electron microprobe X-ray microanalysis (EMPA), using a Jeol model JXA-8600 microanalyser, equipped with a 2 μm diameter electron

0022–2461

beam, operating at 25 k eV and 20 nA. The X-ray fluorescence counts were accumulated for 80 s at each point. Quantitative results with an overall experimental error of about 0.05 at % were obtained using CdTe and ZnTe secondary standards.

A double crystal diffractometer with a Cu X-ray tube aligned in the + / − non-dispersive setting was used to assess the crystalline quality. A high perfection InSb crystal orientated to the (3 3 3) reflection served as a monochromator.

The optical photomicrographs were performed by regular optical microscopy. A Philips SEM model 535 at 25 kV was utilized for the imaging of defects induced in the Zn diffused layer.

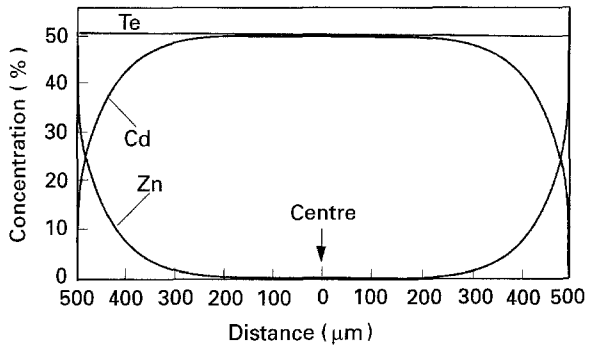

Figure 1 Distribution profiles of Zn, Cd and Te after diffusion, where complete exchange between Zn and Cd has occurred.

The AFM analysis was performed on a digital Instruments Nanoscope II, which has an effective scan range of up to 140 μm. The cantilevers are gold coated silicon nitride and have a force constant of 0.06 $N\,m^{-1}$. Measurements of surface features and in particular the surface roughness were obtained by using the available software and a basic standard calculation [5].

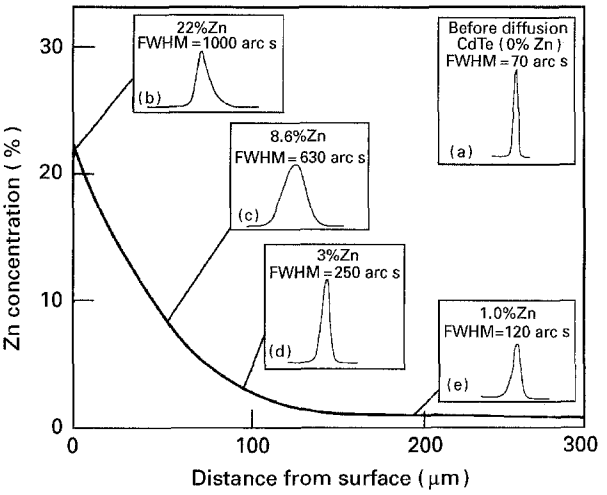

Figure 2 Zn distribution in a wafer after diffusion from Zn depleted reservoir and DCRCs (a) before diffusion, (b) after diffusion on the surface, (c) after removing 50 μm, (d) after removing 90 μm, and (e) after removing 190 μm.

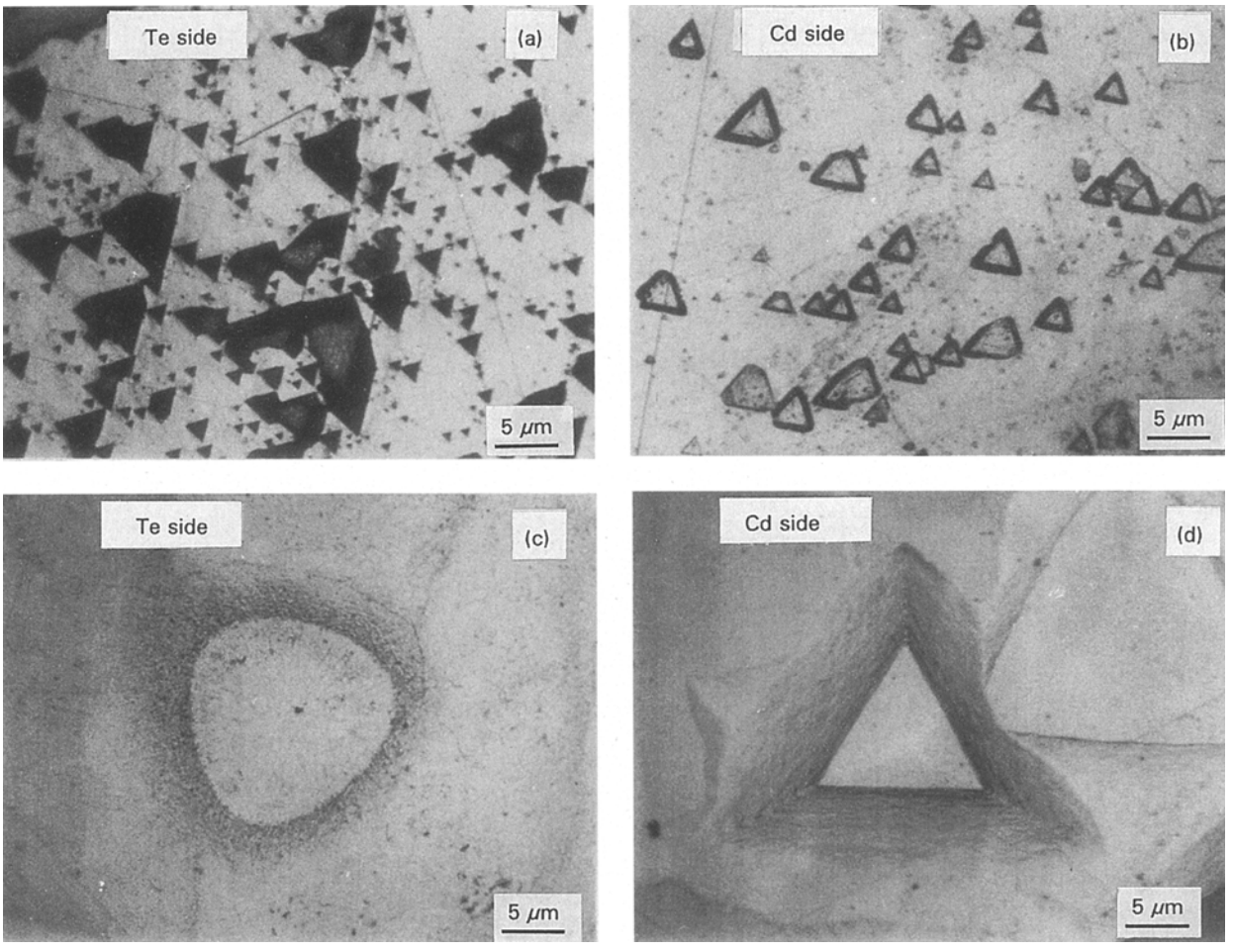

Figure 3 Photomicrographs of surface defects on a CdTe wafer after diffusion. The defects are identified as thermal etch pits on the Te side (a) and (c), and on the Cd side (b) and (d).

3. Results

Fig. 1 shows the typical distribution profiles of Zn, Cd and Te, parallel to the diffusion direction on the cleavage plane {1 1 0} in a (1 1 1) orientated CdTe wafer that was subjected to high temperature diffusion (3 h at 950 °C) in the presence of Zn vapour (15% Zn in CdZn reservoir). It is clearly observed in Fig. 1 that the Zn concentration decreases from the surface towards the centre, where the Cd concentration increases and the Te concentration remains almost constant, around 50%. Such decay profiles indicate a substitutional exchange mechanism between Zn and Cd during the diffusion process, where almost complete transformation of CdTe to ZnTe could be obtained near the surface. The details of the diffusion model and an extensive study of the diffusion parameters have been published recently [2] and are utilized here to calculate the predetermined Zn distribution curve which is further discussed.

Fig. 2 shows the calculated Zn distribution in a wafer that was subjected to diffusion, when the CdZn reservoir had a significantly lower Zn concentration (7% Zn in the CdZn reservoir) and the measured Zn concentration on the surface was 22%.

X-ray double crystal rocking curves (DCRCs) of the (3 3 3) type reflection were measured on the wafer before the diffusion process, after diffusion and after removal of several layers. The DCRCs are shown in Fig. 2, where the different curves are correlated to the Zn concentration which was measured on the surface after removal of a particular layer, the thicknesses of the removed layers are 50, 90 and 190 μm, and are shown in Fig. 2c–e, respectively. These experimental points fit very well within the calculated curve. The variable which is utilized as a quantitative figure is the full width at half maximum (FWHM) of the rocking curves in arc s, the curves with split peaks are indicative for local crystallographic misorientation of different regions in the measured field. It is noted that after removing a layer of about 90 μm, where the Zn concentration is 3%, the FWHM of the DCRC is 250 arc s, which is higher only by a factor of three as compared to that of the sample before diffusion. Fig. 3 shows photomicrographs of surface defects which were observed on the surfaces of two (1 1 1) orientated CdTe wafers. The nature of these defects is identified as thermal etch pits, as a result of the diffusion of Zn at 950 °C. Fig. 3a, b shows the pits on the Te and Cd sides of the wafer, respectively, where the Zn concentration on the surface was 22%. Fig. 3c, d shows the pits in the same sequence of Fig. 3a, b for the second wafer, where the surface Zn concentration is about 10%. The crystallographic symmetry of the thermal etch pits on both sides of the two wafers is similar to the well known chemical etch pits in CdTe and CdZnTe, which can be obtained after polishing and chemical etching in E–Ag1 and E–Ag2 solutions [6]. It should be noted that both wafers were extracted

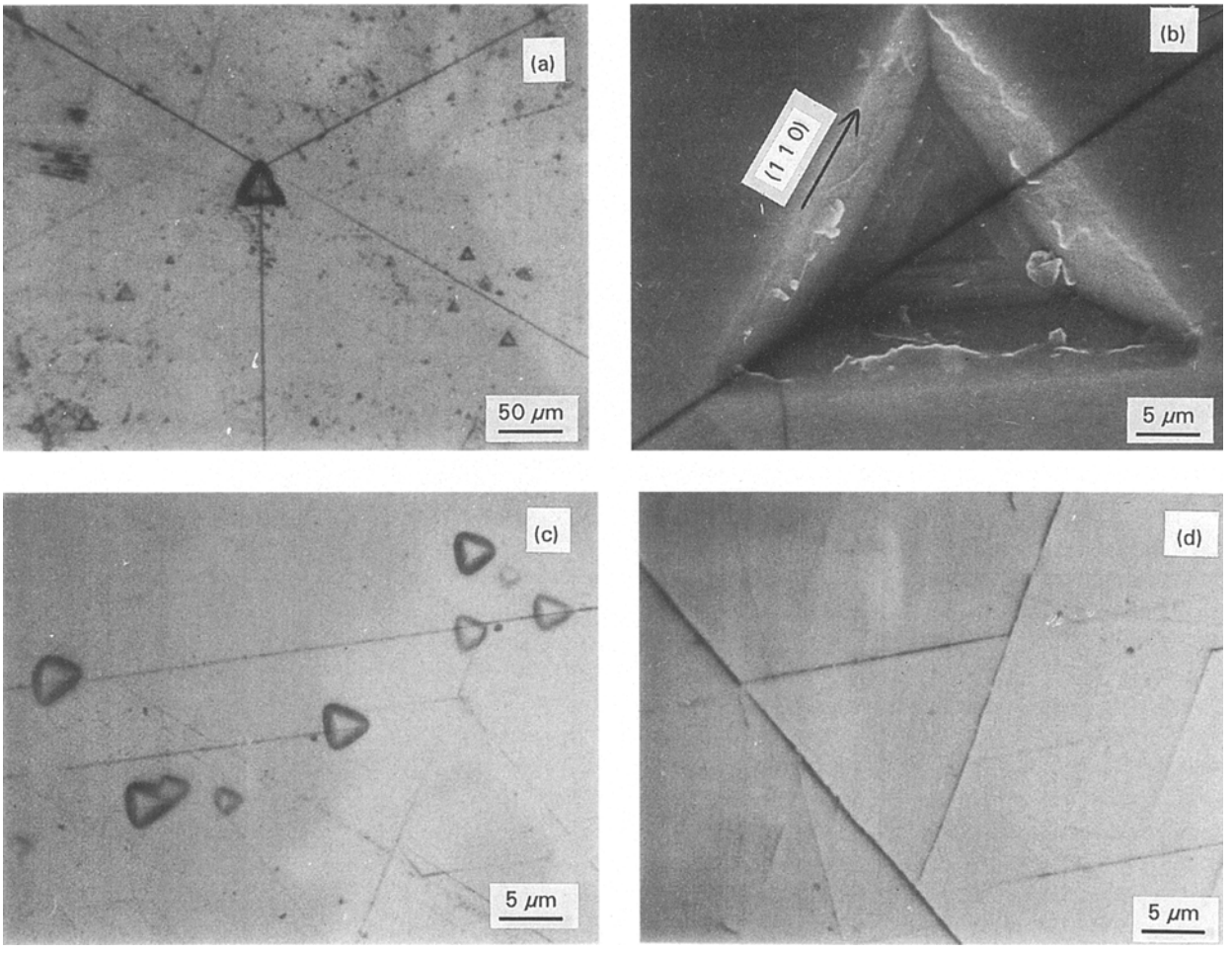

Figure 4 (a) A single thermal etch pit and three-fold slip lines on the Cd side of a (1 1 1) orientated wafer, (b) SEM of a similar pit to Fig. 4a, (c) and (d) are from the same surface of Fig. 4a after polishing 40 and 80 μm from the surface, respectively.

from the same crystal piece and exhibited an identical crystal perfection before the diffusion process. Fig. 4a shows a photomicrograph of a single thermal etch pit, commenced in the vertex of three-fold fine lines on the Cd face of the (1 1 1) orientated wafer. Further, a high resolution image of a thermal etch pit was carried out by SEM and is shown in Fig. 4b, clearly indicating the geometry of the intersection between the pit and the cracking line. The crystallographic direction analysis of this symmetry is further discussed below. Fig. 4c, d shows the photomicrographs on the surface of the Cd side of the wafer shown in Fig. 3b after polishing the surface and removing a step of 40 μm (Fig. 4c) and then a second step of additional 40 μm (Fig. 4d) from the surface. The thermal pit density and the cracking lines gradually decreased. Finally, after polishing a total thickness of about 200 μm, the defective structure was completely removed and the crystalline perfection of the surface, assessed by X-ray DCRC (seen in Fig. 2e), showed a FWHM of 120 arc s, which is only slightly higher than before the diffusion process (FWHM of 70 arc s, seen in Fig. 2a). Fig. 5 shows the photomicrographs of as-cleaved surfaces, (1 1 0) orientated CdTe wafers. Fig. 5a, b shows the edges of the

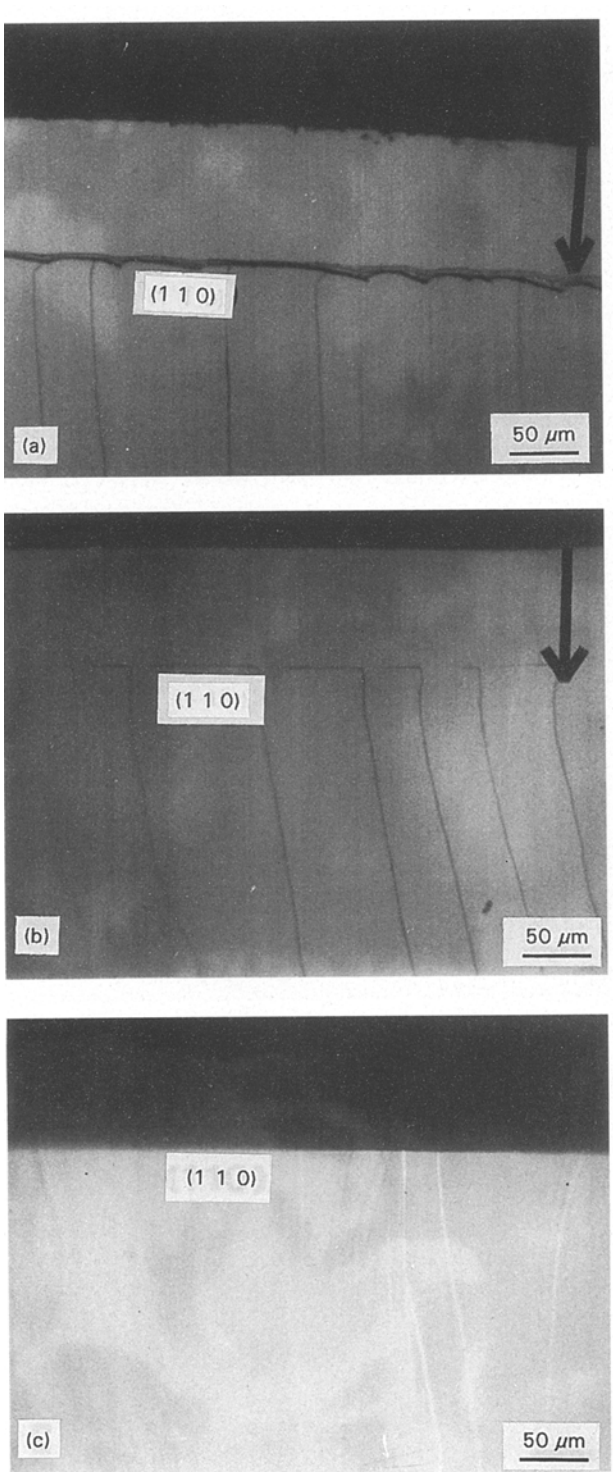

Figure 5 Photomicrographs of an as-cleaved (1 1 0) surface, after diffusion (a) and (b), before diffusion (c).

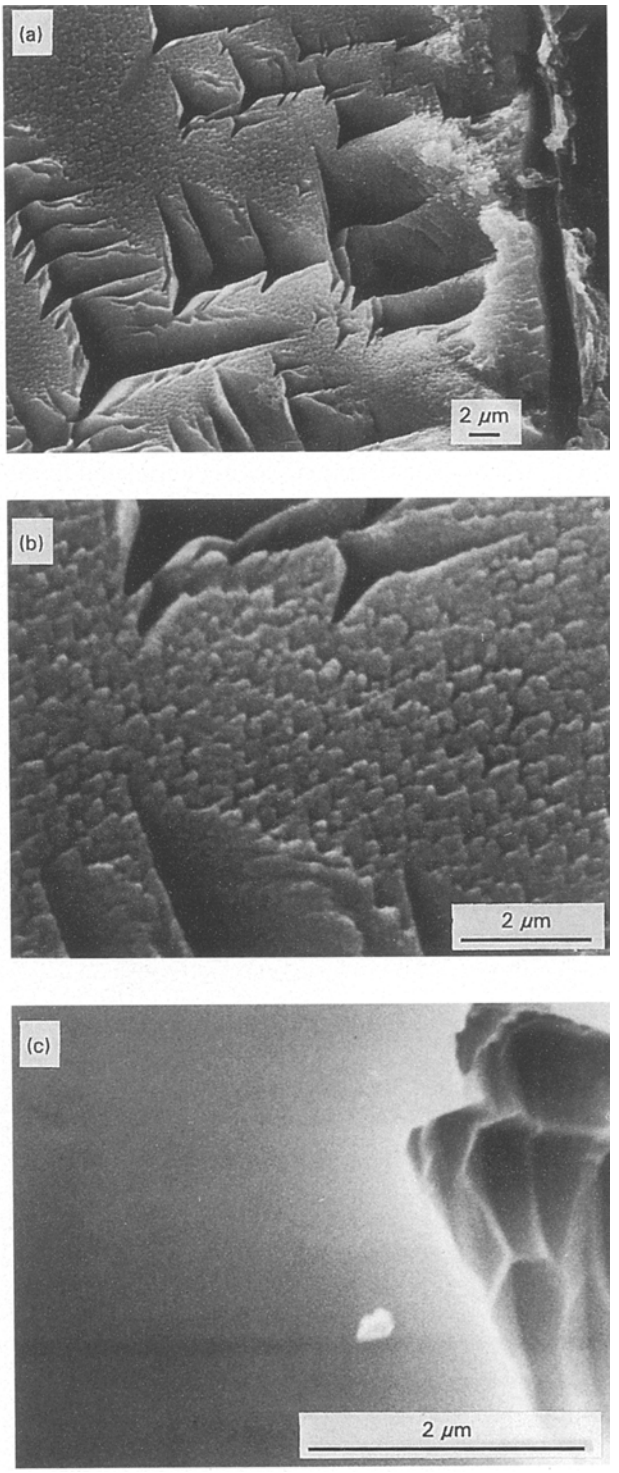

Figure 6 SEM micrographs on cleaved surface of a wafer subjected to diffusion with high Zn concentration, after chemical etching.

cleavage plane, near the two surfaces which are the cross-section of the diffusion plane, parallel to the diffusion directions. The arrows show the diffusion direction through both sides of the wafer and perpendicular to the (1 1 1) plane which is the surface of the wafer. Fig. 5c shows for comparison an as-cleaved surface of a CdTe wafer before diffusion. As can be clearly observed by comparing the cleaved (1 1 0) surfaces of a CdTe (1 1 1) orientated wafer, the cleavage lines in the wafer after diffusion stopped and then turned towards a line parallel to the top surfaces with distances of 100 and 85 μm, in Fig. 5a, b, respectively, while the cleavage lines in Fig. 5c approach the top surface on both sides of the wafer. The distances of 100 and 85 μm indicated above fit the diffusion depth where the Zn concentration is about 2%, which is the beginning of the tail in the Zn decay profile (shown in Fig. 2).

Figs 6 and 7 summarize the SEM observation of structural defects that were revealed on the cleaved surface (1 1 0) after a selective chemical etching process in an E–Ag1 solution for 60 s and then rinsed in methanol. Fig. 6a presents a very high density of extended pits, with size up to 20 μm and a homogeneous substructure of deformed patterns in a CdTe wafer that was subjected to diffusion of Zn at 950 °C for 3 h when the Zn concentration on the surface was 22%. The substructure is shown with higher resolution in Fig. 6b, where the average size of the features is 0.5 μm. Fig. 6a, b was performed just near the surface (seen at the right-hand side of Fig. 6a) of the wafer, which typically exhibits the highest Zn concentration and apparently the mostly deformed region. Fig. 6c shows a remote area, at about 300 μm below the surface in the same {1 1 0} cleavage plane, from which Fig. 6a and b were performed. This area is almost free of pits or any other observable structure. The deformed area shown in Fig. 6c was chosen just for contrast and is not entirely typical for that region. Fig. 7 presents a similar sequence of images to those of Fig. 6, for a CdTe wafer with a lower surface Zn concentration of 10% as compared to 22% of the sample of Fig. 6. A much lower etch pit density was obtained from Fig. 7a as compared to that of Fig. 6a. The very fine substructure can be seen in Fig. 7b on both sides of the large pit, where the remote area in Fig. 7c is similar to the as-cleaved structure. Fig. 8 presents high resolution images of {1 1 0} cleaved surfaces that were carried out by AFM on three samples. Fig. 8a shows an image of 50×50 μm scan area of cleaved surface near the edge of the CdTe sample, before diffusion. No substructure or features were observed, the cracks near and at the centre of the edge are probably a result of cleavage damage; which often occurs. Fig. 8b shows a small area of 1×1 μm within the area shown in Fig. 8a, where the vertical resolution is higher by two orders of magnitude (10 and 1000 nm unit^{-1} in the Z range, respectively). No substructure can be observed, except for several bright dots which may be identified as Te precipitates and jogs, which are identified as cleavage steps. Detailed investigation of this phenomenon has been reported recently elsewhere [3]. Fig. 8c shows an image of an

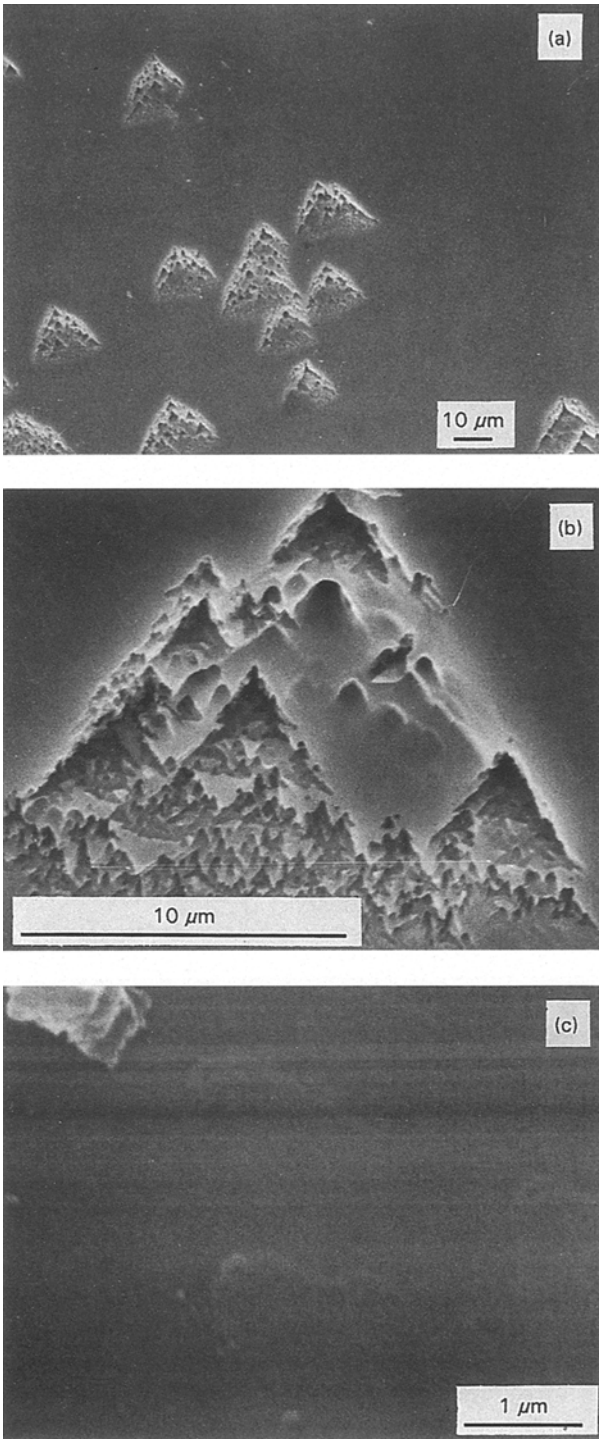

Figure 7 SEM micrographs on cleaved surface of a wafer, subjected to diffusion with low Zn concentration, after chemical etching.

as-cleaved surface in a sample that was subjected to diffusion of Zn with surface concentration of 10%. The image was carried out near the surface, 5 μm below the edge. A rough structure is evident and a surface roughness of 7.44 nm ($\sigma = 1.10$ nm) was calculated. This roughness is considered as highly defected structure and can be attributed to deformation accompanying the diffusion process. The deep line across the image may be a trace of a cleavage step; however, since no significant height difference was measured between the two sides of the line it can be speculated that it is a trace of a structural cracking line, such as the one shown above in Fig. 5. Fig. 8d

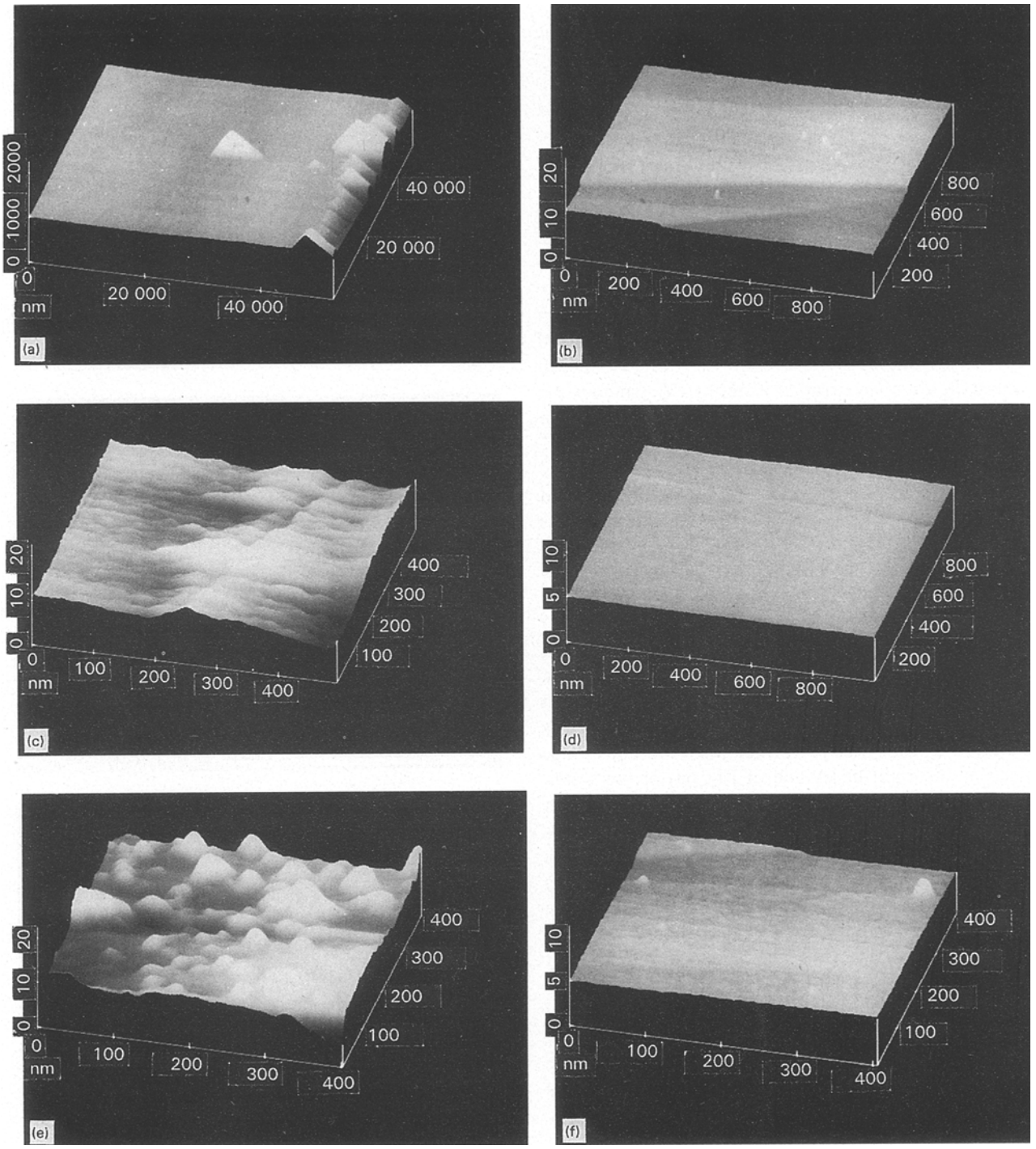

Figure 8 Atomic force microscopy (AFM), high resolution images of as-cleaved surfaces before diffusion (a) and (b), after diffusion with low Zn concentration (c) and (d), after diffusion with high Zn concentration (e) and (f).

shows for comparison an image from the same surface with the same resolution as Fig. 8c, that was taken 400 μm below the surface. An almost atomically flat surface could be obtained, while a roughness of 0.79 nm ($\sigma = 0.07$ nm) was measured, indicating a height of three atomic layers of the $\{1\,1\,0\}$ planes with an interplanar distance of 0.228 nm. Fig. 8e, f shows the AFM images on the cleavage plane, near the edge and remote from the surface, respectively, in a sample with surface Zn concentration of 22%. A very high surface roughness of 12.24 nm ($\sigma = 1.55$ nm) was obtained in a region with distance of 30 μm below the surface, shown in the image of Fig. 8e; while the area remote from the surface, which is shown in Fig. 8f, exhibited almost an atomically flat surface and some traces of an apparent cleavage line.

4. Discussion

The diffusion of Zn vapour into CdTe crystals was investigated recently [2], indicating an exchange mechanism between Cd atoms evaporated from the crystal surface and the diffused Zn atoms provided from the vapour of a CdZn reservoir. A model for the diffusion process has suggested that the evaporation velocity of Cd from the surface is the rate limiting

factor of the process, fitting a mathematical solution for the diffusion equation which considers the sorption–desorption mechanism on the surface [7]. The diffusion process can provide a CdZnTe solid solution in the complete range from CdTe up to ZnTe, as has been shown in Fig. 1. The crystalline structure was analysed by various X-ray methods to assess the lattice constant, as well as the crystalline perfection, indicating that the difffusion process causes a deterioration of crystalline perfection mostly near the surface. Such phenomenon is known to be involved with motion of dislocations as well as generating thermomechanical defects, both contributing to the deformation of the crystal. Quantitatively, the dislocation density was found to be directly proportional to the Zn concentration. The FWHM values of the DCRCs in Fig. 1a show an initial value of 70 arc s on a wafer before diffusion, the FWHM was increased to 1000 arc s after diffusion and then decreased gradually down to 120 arc s. The FWHM ($\Delta\Theta_{1/2}$) values of the DCRCs were found to be in good correlation with the dislocation density, D, in the crystal, calculated by using the equation $D = (\Delta\Theta_{1/2})^2/9\mathbf{b}^2$, where $\mathbf{b}$ is the Burger's vector. The detailed analysis and the correlation with etch pit density in CdZnTe single crystals has been reported recently elsewhere [8].

The crystallographic structure of the defects can be analysed from the thermal etch pits which are shown in Figs 3 and 4. A schematic illustration of a crystallographic model, explaining the orientations and directions of the defects is shown in Fig. 9. The (1 1 1) wafers of CdTe, which were subjected to high temperature diffusion of Zn, exhibited large triangular thermal etch pits with edges of about 10 nm along the $\langle 1\,1\,0\rangle$ direction (see Fig. 4b). Two networks of triangular hatch patterns were also revealed on the surface of the wafers. The first one consisted of thick lines aligned in the $\langle 2\,1\,1\rangle$ direction. In the other, fade lines running along the $\langle 1\,1\,0\rangle$ direction were observed. These lines disappeared only after deep etching (see Fig. 4c, d). The CdZnTe layer formed during the diffusion process has a smaller lattice constant than that of the CdTe layer. Very large lateral stresses are introduced into the CdZnTe layer due to lattice mismatch between the two materials. Dislocations are introduced into the layer, initiating a strain relaxation process, particularly when exceeding a critical thickness. Cracks can be formed along the $\{1\,1\,0\}$ cleavage planes, in thicker layers, with a large lattice mismatch coefficient. A careful examination shows that the triangular hatch patterns on the diffused CdTe surfaces are lying along the intersections of the six $\{1\,1\,0\}$ cleavage planes, existing in the zincblende crystalline system with the (1 1 1) surface plane. The $\langle 2\,1\,1\rangle$ net belongs to $\{1\,1\,0\}$ planes which are perpendicular to the $\{1\,1\,1\}$ surface plane. The lateral stresses introduced via the Zn diffusion process activate the $\langle 1\,1\,1\rangle\{1\,1\,0\}$ slip systems inducing dislocation movement on the different $\{1\,1\,1\}$ slip planes. Reaction or dissociation of dislocations on the $\langle 1\,1\,0\rangle$ intersection line between two crossing $\{1\,1\,1\}$ planes results in immobile stair-rod edge dislocations with Burger's vector of (1/6) $\langle 1\,1\,0\rangle$, which do not lie on a slip plane. These immobile dislocations

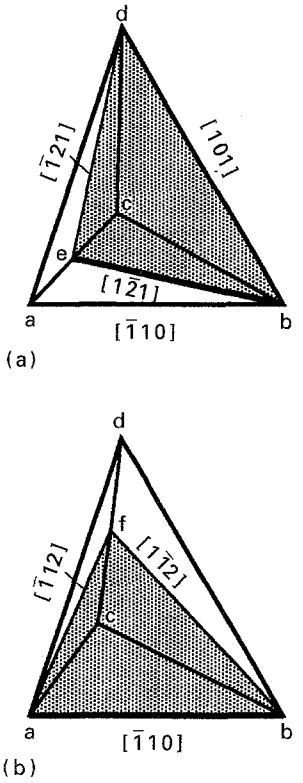

Figure 9 Schematic illustration of a crystallographic model with orientations and directions of the defects: (a) triangle abc represents (1 1 1) plane, triangle bde represents (1 1 0) vertical cleavage plane; (b) triangle abc represents (1 1 1) plane, triangle abf represents (1 1 0) inclined cleavages plane.

serve as obstacles to other moving dislocations. Such reaction and dissociation are given for example by the following reaction

$$(1/6)\,[\bar{1}\,\bar{2}\,\bar{1}] + (1/6)[2\,1\,1] \rightarrow (1/6)\,[1\,\bar{1}\,0]$$

$$(1/6)\,[\bar{2}\,1\,1] \rightarrow (1/6)[\bar{1}\,2\,1] + (1/6)\,[\bar{1}\,\bar{1}\,0]$$

Pile up of dislocations eventually yields cracks parallel to the $\{1\,1\,0\}$ planes. Reaction between dislocations moving on $\{1\,1\,1\}$ planes inclined to the surface yields perpendicular $\{1\,1\,0\}$ cleavage planes which intersect the (1 1 1) surface plane along $\langle 2\,1\,1\rangle$ directions. However, when one of the slip planes is parallel to the surface, the resulting (1 1 0) cleavage plane is inclined to the surface. Such planes intersect the surface at a $\langle 1\,1\,0\rangle$ type direction. The resolved shear stress due to the Zn diffusion is proportional to $\cos\Theta\cos\varphi$, where Θ is the angle between the stress axis and the slip direction, and φ is the angle between the stress axis and the normal to the slip plane. It is clear that $\cos\Theta$ for the $\{1\,1\,1\}$ plane parallel to the surface is smaller, thus the resolved shear stress is much smaller in this plane, resulting in weaker cleavage traces in the $\langle 1\,1\,0\rangle$ directions. The structural defects were further analysed in the cross-section, on the (1 1 0) cleaved surface which is parallel to the diffusion direction and perpendicular to the surface. The optical photomicrographs show typical cleavage patterns (see Fig. 5). However, the cleavage lines in the diffused sample exhibited unexpected phenomena (bending near the surface) which may be attributed to the mechanical stresses as

a result of the difference in the lattice parameter in those regions. The high resolution SEM analysis has shown the preferred orientation defects only after a selective etching process. Whereas no substructure could be observed by SEM on the untreated as-cleaved surface. However, the AFM analysis was found to be very efficient in assessing the deformed structure near the edges of the cross-section, (1 1 0) surfaces, indicating surface roughness as a quantitative measure for defect formation which correlates the Zn concentration in the analysed sample.

References

1. N. ASLAM, E. D. JONES, T. C. Q. NOAKES, J. B. MULLIN and A. F. W. WILLOUGHBY, *J. Cryst. Growth* **117** (1992) 249.
2. M. AZOULAY, M. SINVANI, M. MIZRACHI and H. FELDSTEIN, ibid. **137** (1994) 208.
3. M. AZOULAY, M. A. GEORGE, W. E. COLLINS and E. SILBERMAN, *J. Vac. Sci. & Technol.* **B11** (1993) 148.
4. M. AZOULAY, A. RAIZMAN, G. GAFNI and M. ROTH, *J. Cryst. Growth* **101** (1990) 256.
5. R. C. CHAPMAN, P. SMITH, R. P. ADU, G. E. MCGUIRE, C. CANOVAI and C. OSBURN, *J. Vac. Sci. & Technol.* **B10** (1992) 1329.
6. M. IVOVE, I. TERAMOTO and S. TAKAYANAGI, *J. Appl. Phys.* **33** (1962) 8.
7. J. CRANK, "The Mathematics of diffusion" (Clarendon, Oxford, 1956) pp. 56–57.
8. M. AZOULAY, S. ROTTER, G. GAFNI and M. ROTH, *J. Cryst. Growth* **116** (1992) 515.

Received 24 October 1994
and accepted 11 April 1995